

Critical issues in the determination of the bentonite cation exchange capacity

Original

Critical issues in the determination of the bentonite cation exchange capacity / Dominijanni, A.; Fratalocchi, E.; Guarena, N.; Manassero, M.; Mazzieri, F.. - In: GÉOTECHNIQUE LETTERS. - ISSN 2045-2543. - STAMPA. - 9:(2019), pp. 205-210. [10.1680/jgele.18.00229]

Availability:

This version is available at: 11583/2770573 since: 2019-12-05T11:09:05Z

Publisher:

ICE Publishing

Published

DOI:10.1680/jgele.18.00229

Terms of use:

This article is made available under terms and conditions as specified in the corresponding bibliographic description in the repository

Publisher copyright

(Article begins on next page)

**Critical issues in the determination of the bentonite cation exchange capacity for the
assessment of the macroscopic density of the solid electric charge**

By

Dominijanni A.* , Fratalocchi, E., Guarena N., Manassero M., Mazzieri F.

• Abstract

The swelling pressure and transport properties of bentonites are controlled by the electric charge density of solid particles, which is commonly estimated from the laboratory measurement of the cation exchange capacity (CEC). However, the standard ammonium displacement method for CEC determination does not take into account the fabric changes that occur in bentonites under exposure to high salt concentration solutions. A series of laboratory tests was conducted to assess the relevance of such a critical issue, by varying the concentration of the extracting KCl solution with respect to that of the standard test. The obtained results show that the release of the adsorbed ammonium cations depends on the bentonite fabric, which is controlled by the KCl concentration. As a consequence, the ammonium displacement method may provide an unrepresentative estimate of the CEC of bentonites. The methylene blue titration method, despite its apparently more limited accuracy, instead seems to provide a more reliable estimation of the CEC, as the bentonite fabric is maintained dispersed during the test.

Keywords chosen from the ICE Publishing list

Geosynthetic application, Landfills, Waste management & disposal

List of notations

α	empirical coefficient of the fabric boundary surface equation
β	empirical coefficient of the fabric boundary surface equation
ρ_{sk}	solid-phase density
b_n	average half-distance between the platelets in the tactoid
c_0	reference molar concentration in the fabric boundary surface equation
c_s	salt molar concentration
$\bar{c}_{sk,0}$	molar concentration per unit solid volume of the solid skeleton electric charge
CEC	cation exchange capacity
d_d	d_{Stern}/b_n
d_{Stern}	thickness of the Stern Layer around the external surface of the tactoid
e	total void ratio
e_m	micro-void ratio
f_{Stern}	fraction of cations adsorbed in the Stern layer
H	height of the bentonite layer in the filtration apparatus of the ammonium displacement method
k	hydraulic conductivity of the bentonite layer in the filtration apparatus of the ammonium displacement method
$N_{I,AV}$	average number of lamellae per tactoid
$N_{I,AV0}$	empirical coefficient of the fabric boundary surface equation

S total specific surface of bentonite
u_{sw} swelling pressure

1 Introduction

2 The transport properties and mechanical behaviour of clay soils with a high specific surface,
3 such as bentonites, are governed by the microscopic interactions that occur between the
4 electrically charged solid particles and the ions that are contained in the pore solution (Lambe,
5 1960; Groenevelt and Bolt, 1969; Sridharan and Rao, 1973; Mitchell, 1991; Moyne and Murad,
6 2002; Mitchell and Soga, 2005; Guimarães et al., 2013; Musso et al., 2017; Revil, 2017a,
7 2017b; Delage, 2019).

8 Bentonites can have either a dispersed fabric, in which clay particles are present as well
9 separated montmorillonite units, or an aggregated structure that consists of packets of particles,
10 or tactoids, within which several clay platelets are in a parallel array. The formation of tactoids is
11 determined by a reduction in the electrical repulsive forces among the clay particles, which is
12 mainly induced by an increase in the salt concentration or a decrease in the solvent dielectric
13 constant of the pore solution.

14 The expected performances of bentonites can be assessed in field applications through
15 physics-based models, which relate the macroscopic constitutive parameters, including
16 hydraulic conductivity, chemico-osmotic efficiency, diffusion coefficient and swelling pressure, to
17 microscopic fabric parameters, such as the average number of montmorillonite lamellae per
18 tactoid, $N_{i,AV}$ (Dominijanni and Manassero, 2012; Shackelford et al., 2019).

19 Manassero (2017) described a physics-based model that was obtained by volume averaging the
20 equations that govern the electric potential distribution, the water flow and the ion transport at
21 the pore scale, and by imposing the condition of macroscopic thermodynamic equilibrium
22 between the pore solution and the external bulk solutions in contact with the bentonite at its
23 boundaries (Dominijanni and Manassero, 2005, 2012; Dominijanni et al., 2006, 2013, 2018).

24 On the basis of such a theoretical approach, the microscopic (pore scale) properties of
25 bentonites are taken into account through a single fundamental parameter, that is the molar
26 concentration per unit solid volume of the solid skeleton electric charge, $\bar{c}_{sk,0}$. This parameter is
27 related to the cation exchange capacity, CEC, as follows (Dominijanni and Manassero, 2012):
28

$$\bar{c}_{sk,0} = \frac{1 - f_{Stern}}{N_{i,AV}} \cdot CEC \cdot \rho_{sk} \quad (1)$$

where ρ_{sk} is the solid-phase density ($\approx 2700 \text{ kg/m}^3$) and f_{Stern} is the fraction of cations immobilized in the so-called Stern layer ($\approx 0.75\text{--}0.95$).

Although CEC determination alone is not sufficient to allow an evaluation of $\bar{c}_{sk,0}$, it plays a fundamental role in relating the physical and chemical properties of bentonite at the pore scale to the macroscopic constitutive parameters. For this reason, a series of experimental tests has been conducted to assess the reliability of the most commonly used CEC measurement methods, including the ammonium displacement method and the methylene blue titration (MB) method.

2. Materials and methods

2.1 Bentonite

The powdered bentonite used in this study comes from the same lot and was subjected to the same cyclic-squeezing procedure as in Puma et al. (2015) to remove soluble salts prior to further testing. The main properties of the bentonite are listed in Table 1.

2.2 Testing procedures

As far as the ammonium displacement method is concerned, the CEC was determined according to the ASTM D7503-18 procedure, except for the KCl solutions that were used in the final extraction step: in addition to the 1 M KCl solution (standard procedure), extracting solutions with different KCl concentrations (4.5 M, 0.1 M, 0.05 M, 0.025 M, 0.01 M, 0.0025 M, 0.001 M) were used together with distilled water (DW) to investigate the effect of changes in the bentonite fabric on the CEC results. The tests were generally performed in duplicate for each extracting solution.

The MB test was carried out following the procedure outlined in EUBA (2002). The method is a rapid qualitative procedure that is used in industry for routine quality controls, which provides a measure of the accessible anionic sites in a condition of enhanced dispersion of the clay. This

dispersion is obtained by bringing the bentonite suspension to the boil and subsequently titrating the suspension with an anionic dye (methylene blue).

3. Test results

The CEC measurement results are listed in Table 2 and plotted in Figure 1. The solid symbols in Figure 1 represent the CEC values obtained from the ammonium release measurements. The values obtained using DW are plotted at 0.0001 M KCl concentration. Considering the average of the measurements for each extracting solution concentration, the maximum value of CEC measured with ammonium was 75.3 meq/100g, which was obtained for the 0.1 M KCl solution (the value of 103 meq/100g for the third replicate at 0.1 M KCl was considered to be an outlier of the dataset and, therefore, neglected). As a result, the maximum CEC value obtained with ammonium was lower than the values obtained with the MB tests (97 and 104 meq/100g; for the sake of simplicity the mean value is plotted in Figure 1). The results suggest that the measured CEC depends on the aggregation state of the bentonite particles. The MB test seems to provide an upper bound of the measured CEC due to the disperse state of the bentonite, which enhances the accessibility of exchange sites with respect to the state of aggregation obtained in the standard test. Despite some scatter in the results, the average CEC versus KCl concentration tends to be practically constant for $KCl > 0.1\text{ M}$, thus suggesting a similar aggregation state of bentonite particles. As the KCl concentration decreased ($< 0.1\text{ M}$), the CEC calculated from the released ammonium also decreased. It should be considered that the amount of K cations available for exchange also decreased. The maximum theoretically measurable CEC, as calculated from the available potassium, is also shown in Figure 1. The measured CEC values for low ($< 0.02\text{ M}$) to practically zero (DW) KCl concentrations are in the 13.9 - 23.9 meq/100g range, that is higher than the theoretically predicted values based on the available potassium. A blank test (performed without soil and using a 1 M KCl solution) showed that the ammonium residue in the apparatus at most accounts for 1.3 meq/100g. Therefore, the measured CEC suggests a release of ammonium from the clay that is not related to the adsorption of potassium. According to the test method, washing the clay with isopropanol should remove the excess unbound ammonium acetate; however, the test results suggest that some residual ammonium remains in the clay. A replicate test was performed using 0.0025 M

KCl solution and a double wash with isopropanol (240 ml instead of 120 ml), but no significant difference in the measured CEC was observed (Table 2). Therefore, the test results suggest that, even after washing with isopropanol, some unbound ammonium remains entrapped in the bentonite layer. Filtration with low concentration (< 0.02 M KCl) solutions induces a change in bentonite fabric during the test, namely swelling and reorganisation, whereby the release of ammonium is favoured. This is reflected, at the macroscopic scale, by an increase in the average height of the bentonite film that forms in the filtration apparatus, H , at the end of the tests, and a corresponding decrease in the hydraulic conductivity, k . The k value was estimated from the observed flow rate of the filtrate during the addition of the final 50 ml of the extracting solution and from the hydraulic gradient that was established across the bentonite film during filtration. H was equal to 2.5 mm and the average k was estimated to be about 10^{-7} m/s with the 1 M KCl solution (standard procedure), whereas H was 8 mm and k was about 10^{-9} m/s with DW.

4. Discussion

The observed changes in the hydraulic conductivity of bentonite suggest that the CEC variation, as a function of the extracting KCl solution concentration, can be related to fabric modifications. Manassero et al. (2016, 2018), Dominijanni et al. (2017) and Manassero (2017) modelled bentonite fabric modifications through a fabric boundary surface (FBS), whereby the average number of lamellae per tactoid, $N_{i,AV}$, is related to the salt concentration, c_s , and the micro-void ratio, e_m , which in turn is obtained by subtracting the void space between the platelets of the tactoids from the total void space.

A first phenomenological formulation of FBS was proposed by Manassero et al. (2016):

$$N_{i,AV} = N_{i,AV0} + \frac{\alpha}{e_m} \cdot \left(\frac{c_s}{c_0} + 1 \right) + \beta \cdot e_m \cdot \left[1 - \exp\left(-\frac{c_s}{c_0} \right) \right] \quad (2)$$

where c_0 represents the reference molar concentration ($= 1$ M) and $N_{i,AV0}$, α and β are non-dimensional empirical parameters.

The micro-void ratio, e_m , in Eq. 2 can be derived from the total void ratio, e , through the following equation:

$$e_m = \frac{e \cdot N_{i,AV} - S \cdot \rho_{sk} \cdot b_n (N_{i,AV} + d_d - 1)}{N_{i,AV}} \quad (3)$$

where b_n is the average half-distance between the platelets in the tactoid (≈ 0.4 nm), S is the total specific surface (≈ 700 m²/g) and d_d is the thickness of the Stern Layer divided by b_n (≈ 4).

Inserting Eq. 3 into Eq. 2 the number of lamellae per tactoid is related to the total void ratio and the salt concentration through a cubic equation, which can be solved analytically or numerically for given values of the parameters $N_{i,AV0}$, α , β , S , ρ_{sk} , b_n and d_d .

Although a sufficient number of experimental data is not available for the tested bentonite to determine the FBS parameters, a qualitative analysis was conducted by using the calibration performed by Manassero (2017) on the hydraulic conductivity experimental results obtained by Petrov and Rowe (1997) on a needle-punched geosynthetic clay liner (GCL), which provided $N_{i,AV0} = 1.56$, $\alpha = 8.82$, $\beta = 10.01$. A plot of the corresponding FBS in the space of the variables $N_{i,AV}$, e_m and c_s is shown in Figure 2. Such an FBS can be regarded as suitable for the analysis of the obtained laboratory data, as the features of the bentonite in the GCL are similar to the ones of the tested bentonite (Table 1) and the GCL hydraulic conductivity is not expected to be influenced by the presence of needle-punched fibres, at least in the range of low salt concentrations (< 0.1 M KCl solution) (Puma et al., 2015).

The ability of the proposed FBS to accurately model microstructural changes was verified using a series of experimental results from the literature that included direct measurements of $N_{i,AV}$, on bentonites with similar properties to the ones of the bentonite tested in the present study (Table 1). The values of $N_{i,AV}$, which were estimated directly from the ratio of the intra-tactoid to the inter-tactoid pore-space by means of Small Angle X-Ray Scattering Spectroscopy (Muurinen et al., 2013) and Nuclear Magnetic Resonance techniques (Muurinen et al., 2013; Ohkubo et al., 2016), are shown to be in good agreement with the FBS predictions in Figure 3, for a salt concentration $c_s = 0.1$ M.

The total void ratio was estimated, during the washing phase with isopropanol, from the measurement of the bentonite layer thickness to be about 4 and, as a result, $N_{i,AV}$ is calculated through the FBS equation to be about 4.74, assuming $c_s = 0$ as a consequence of the complete removal of the pore aqueous solution.

The relation between $N_{i,AV}$ and the KCl concentration, c_s , provided by the FBS for the values of the bentonite void ratio that were estimated at the end of the ammonium displacement tests (Table 2) is shown in Figure 4. The value of the KCl concentration corresponding to $N_{i,AV} = 4.74$ is equal to about 0.027 M. As a result, the bentonite is expected to swell during the KCl solution filtration phase and assume a more dispersed fabric when the KCl concentration is lower than 0.027 M, while it is expected to flocculate and assume a more aggregated fabric when the KCl concentration is higher than 0.027 M. Such a theoretical threshold value of the KCl concentration is very close to the experimentally found value of 0.02 M, below which the released ammonium overcomes the available potassium.

This qualitative result suggests an interpretation of the CEC data that were obtained from the ammonium release measurements. After the washing phase with isopropanol, a portion of mobile ammonium was not removed because of the presence of pores that are less accessible to the advection flux. When the KCl concentration of the extracting solution was lower than about 0.02 M, the dispersion of the bentonite allowed the mobile ammonium ions to be released by opening such pores. Instead, when the KCl concentration of the extracting solution was higher than about 0.02 M, the bentonite flocculated and created additional less accessible pore voids. The potassium cations only had access to a limited portion of the available pores for the highest values of the KCl concentration (≥ 1 M), and, as a result, the exchanged ammonium ion measurements underestimated the effective bentonite CEC.

5. Conclusions

The tests performed by varying the KCl solution concentrations showed that the CEC measurements based on ammonium release are influenced by bentonite fabric modifications and may provide an unreliable estimation of the effective density of the exchangeable sites of the bentonite. For this reason, the ammonium displacement method does not seem to be

sufficiently accurate to assess the fundamental fabric parameters of coupled hydro-chemo-mechanical models, such as the one proposed by Manassero et al. (2016). The experimental swelling pressure data obtained by Dominijanni et al. (2013) for a saturated sodium bentonite at a void ratio of 4.26 are compared in Figure 5, by way of example, with the theoretical predictions that are obtained by determining $\bar{c}_{sk,0}$ from the measurement of CEC through Eq. 1, with a constant $N_{i,AV}$ value ($N_{i,AV} = 3$) for the investigated range of low salt concentrations (Manassero, 2017). The theoretical curve derived from the average CEC provided by the standard ammonium displacement method underestimates the experimental data to a great extent, whereas an acceptable fitting is obtained when the average CEC value provided by the methylene blue titration method is used. As a result, the methylene blue titration method, which is used in industry for routine quality controls, seems to be able to provide a more reliable estimation of CEC, despite its apparently more limited accuracy, as the bentonite fabric is maintained dispersed during the test.

References

- ASTM D7503-18 Standard Test Method for Measuring the Exchange Complex and Cation Exchange Capacity of Inorganic Fine-Grained Soils.
- Delage P (2019) Micro-macro effects in bentonite engineered barriers for radioactive waste disposal. In: Zhan L, Chen Y and Bouazza A (Eds.) Proceedings of the 8th International Congress on Environmental Geotechnics, Hangzhou, China; 28 October - 1 November 2018. Springer, Singapore, pp. 61-80.
- Dominijanni A and Manassero M (2005) Modelling osmosis and solute transport through clay membrane barriers. In: Alshawabkeh A, Benson CH, Culligan PJ, Evans JC, Gross BA, Narejo D, Reddy KR, Shackelford CD and Zornberg JG (Eds) Proceedings of the Geo-Frontiers Congress, Austin, Texas (USA), 24-26 January 2005. American Society of Civil Engineers, Reston, Virginia (USA), pp. 349-360.
- Dominijanni A and Manassero M (2012) Modelling the swelling and osmotic properties of clay soils. Part II: The physical approach. *International Journal of Engineering Science* 51: 51-73.
- Dominijanni A, Guarena N and Manassero M (2018) Laboratory assessment of semi-permeable properties of a natural sodium bentonite. *Canadian Geotechnical Journal* 55(11): 1611-1631.
- Dominijanni A, Manassero M and Puma S (2013) Coupled chemical-hydraulic-mechanical behaviour of bentonites. *Géotechnique* 63(3): 191-205.
- Dominijanni A, Manassero M and Vanni D (2006) Micro/macro modeling of electrolyte transport through semipermeable bentonite layers. In: Thomas HR (Ed.) Proceedings of the 5th International Congress on Environmental Geotechnics, Cardiff, Wales (UK), 26-30 June 2006. Thomas Telford, London, England (UK), vol. 2, pp. 1123-1130.
- Dominijanni A, Manassero M, Boffa G and Puma S (2017) Intrinsic and state parameters governing the efficiency of bentonite barriers for contaminant control. In: Ferrari A and Laloui L (Eds.) Proceedings of the International Workshop on Advances in Laboratory Testing and Modelling of Soils and Shales, Villars-sur-Ollon, Switzerland, 18-20 January 2017. Springer International Publishing AG, Cham, Switzerland, pp. 45-56.
- EUBA - European Bentonite Association (2002) Methodology for the determination of the methylene blue value of bentonite.

216 Groenevelt PH and Bolt GH (1969) Non-equilibrium thermodynamics of the soil-water system.
 217 Journal of Hydrology 7(4): 358-388.

218 Guimarães LDN, Gens A, Sánchez M and Olivella S (2013) A chemo-mechanical constitutive
 219 model accounting for cation exchange in expansive clays. *Géotechnique* 63(3): 221-234.

220 Lambe TW (1960) A mechanistic picture of shear strength in clay. In *Proceedings of the*
 221 *Research Conference on Shear Strength of Cohesive Soil*, Boulder, Colorado (USA), June
 222 1960. American Society of Civil Engineers, New York (USA), pp. 555–580.

223 Manassero M, Dominijanni A and Guarena N (2018) Modelling hydro-chemo-mechanical
 224 behaviour of active clays through the fabric boundary surface. In: *Proceedings of China-*
 225 *Europe Conference on Geotechnical Engineering*, Vienna, Austria, 13-16 August 2018.
 226 Springer, Cham, Switzerland, pp. 1618-1626.

227 Manassero M, Dominijanni A, Fratalocchi E, Mazzieri F, Pasqualini E and Boffa G (2016) About
 228 state parameters of the active clays. In: *Proceedings of the Special symposium honoring*
 229 *D.E. Daniel, Geo-Chicago 2016*, 14-18 August 2016, Chicago, Illinois (USA), pp. 99-110.

230 Manassero M. (2017) On the fabric and state parameters of active clays for contaminant control
 231 (2nd ISSMGE Kerry Rowe Lecture). In: Lee W and Lee J-S, Kim H-K and Kim D-S (Eds.)
 232 *Proceedings of the 19th International Conference of Soil Mechanics and Geotechnical*
 233 *Engineering*, Seoul, Korea, 17-22 September 2017, pp. 167-189.

234 Mitchell JK (1991) *Conduction phenomena: from theory to geotechnical practice*. *Géotechnique*
 235 41(3): 299-340.

236 Mitchell JK and Soga K (2005) *Fundamentals of soil behavior* (3rd Edition). John Wiley & Sons,
 237 New York (USA).

238 Moyne C and Murad MA (2002). Electro-chemo-mechanical couplings in swelling clays derived
 239 from a micro/macro-homogenization procedure. *International Journal of Solids and*
 240 *Structures* 39(25): 6159-6190.

241 Musso G, Cosentini, RM, Dominijanni A., Guarena N and Manassero M (2017) Laboratory
 242 characterization of the chemo-hydro-mechanical behaviour of chemically sensitive clays.
 243 *Rivista Italiana di Geotecnica*, vol. 2017 (3): 22-47.

244 Muurinen A, Carlsson T and Root A (2013) Bentonite pore distribution based on SAXS, chloride
 245 exclusion and NMR studies. *Clay Minerals* 48 (2): 251-266.

246 Ohkubo T, Ibaraki M, Tachi Y and Iwadate Y (2016) Pore distribution of water-saturated
 247 compacted clay using NMR relaxometry and freezing temperature depression; effects of
 248 density and salt concentration. *Applied Clay Science* 123: 148-155.
 249 Petrov RJ and Rowe RK (1997) Geosynthetic clay liner (GCL) - chemical compatibility by
 250 hydraulic conductivity testing and factors impacting its performance. *Canadian Geotechnical*
 251 *Journal* 34: 863-885.
 252 Puma S, Dominijanni A, Manassero M and Zaninetta L (2015) The role of physical
 253 pretreatments on the hydraulic conductivity of natural sodium bentonites. *Geotextiles and*
 254 *Geomembranes* 43: 263-271.
 255 Revil A (2017a) Transport of water and ions in partially water-saturated porous media. Part 1.
 256 Constitutive equations. *Advances in Water Resources* 103: 119-138.
 257 Revil A (2017b) Transport of water and ions in partially water-saturated porous media. Part 2.
 258 Filtration effects. *Advances in Water Resources* 103: 139-152.
 259 Shackelford CD, Lu N and Malusis MA (2019) Research challenges involving coupled flows in
 260 geotechnical engineering. In: Lu N and Mitchell JK (Eds.) *Geotechnical Fundamentals for*
 261 *Addressing New World Challenges*. Springer.
 262 Sridharan A and Rao VG (1973) Mechanisms controlling volume change of saturated clays and
 263 the role of the effective stress concept. *Géotechnique* 23(3): 359-382.
 264
 265

Table captions

Table 1. Main properties of the bentonite used in this study and comparison with the data of similar bentonites from the literature (Petrov and Rowe, 1997; Muurinen et al., 2013; Ohkubo et al., 2016) (DW = distilled water).

Table 2. CEC values obtained in the study.

Figure captions

Figure 1. CEC values determined with the ammonium acetate method using different KCl solutions in the final stage of the test and comparison with MB results.

Figure 2. Plot of the fabric boundary surface (FBS) in the three-dimensional space of the variables: average number of lamellae per tactoid, $N_{i,AV}$, micro-void ratio, e_m , and salt molar concentration, c_s .

Figure 3. Comparison between the average number of lamellae per tactoid provided by the Fabric Boundary Surface (continuous line) and the experimental results taken from the literature.

Figure 4. Average number of lamellae per tactoid of the bentonite as a function of the concentration of the extracting KCl solution. The arrows indicate the KCl concentration ($c_s = 0.027$ M) that corresponds to $N_{i,AV} = 4.74$, i.e. the average number of lamellae per tactoid after the washing phase with isopropanol ($c_s = 0$).

Figure 5. Comparison between the swelling pressure of bentonite, as theoretically predicted on the basis of the average CEC value derived from the methylene blue titration method [curve (a) – $CEC = (97.4 + 104)/2 = 100.7$ meq/100g] and the standard ammonium displacement method [curve (b) – $CEC = (73.2 + 60.7)/2 = 66.9$ meq/100g], and the experimental data obtained by Dominijanni et al. (2013) (closed circles).

Table 1. Main properties of the bentonite used in this study and comparison with the data of similar bentonites from the literature (Petrov and Rowe, 1997; Muurinen et al., 2013; Ohkubo et al., 2016) (DW = distilled water).

Property	This Study	Petrov and Rowe (1997)	Muurinen et al. (2013)	Ohkubo et al. (2016)
Smectite content (%)	> 98	91	84	> 98
Prevalent adsorbed cation	Na ⁺	Na ⁺	Na ⁺	Na ⁺
Liquid Limit to DW (%)	525	530	-	-
CEC (meq/100g)	97 - 104 ^(a)	85.8 ^(b)	80 - 88 ^(c)	-
Hydraulic conductivity to DW (m/s)	8.0×10 ⁻¹² ^(d)	1.2×10 ⁻¹¹ ^(e)	5.0×10 ⁻¹² ^(f)	-

^(a) measured through the methylene blue titration method

^(b) measured through the Ag-Thiourea exchange for Na⁺ and K⁺, the KCl exchange for Mg²⁺ and Ca²⁺

^(c) measured through the Cu(II)-Triethylenetetramine exchange method

^(d) measured at a 27.5 kPa confining effective stress

^(e) measured at a 35 kPa confining effective stress

^(f) measured at a bulk dry density equal to 517 kg/m³

13 Table 2. CEC values obtained in this study.

		Test 1 (meq/100 g)	Test 2 (meq/100 g)	Test 3 (meq/100 g)	Note
<u>ASTM D7035</u> (standard and modified procedure)	Estimated bentonite void ratio, e ^(*)				
DW	14	17.5	20.4	13.9	
0.001 M	12	18.9	-	-	
0.0025 M	12	21.4	17.7	-	
0.0025 M	12	21.5	-	-	Double wash with isopropanol
0.01 M	10	23.9	18.4	-	
0.025 M	8	42.0	45.4	-	
0.05 M	7	60.0	63.4	-	
0.1 M	6	76.2	74.4	103	
1 M (standard)	4	73.2	60.7	-	
1 M (standard)	-	1.3	-	-	Blank test (no soil)
4.5 M	3	63.0	76.3	-	
<u>Methylene Blue</u> (EUBA)					
	-	97.4	104	-	

14 ^(*) total void ratio estimated from the detection of the bentonite layer thickness within the filtration
15 apparatus at the end of the ammonium displacement tests

16

17

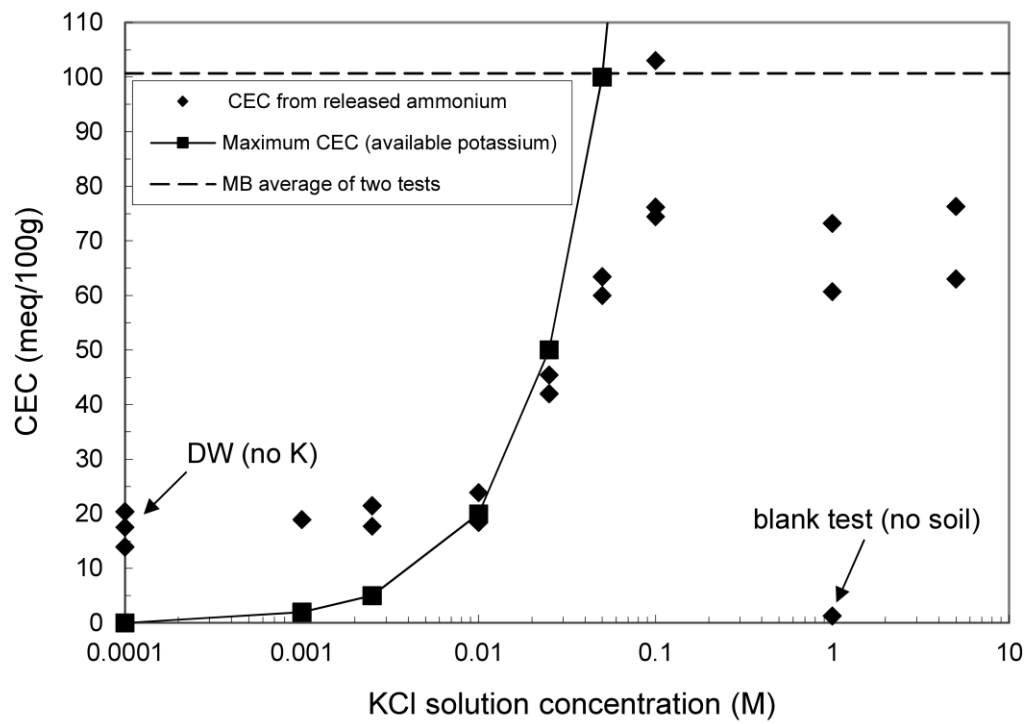
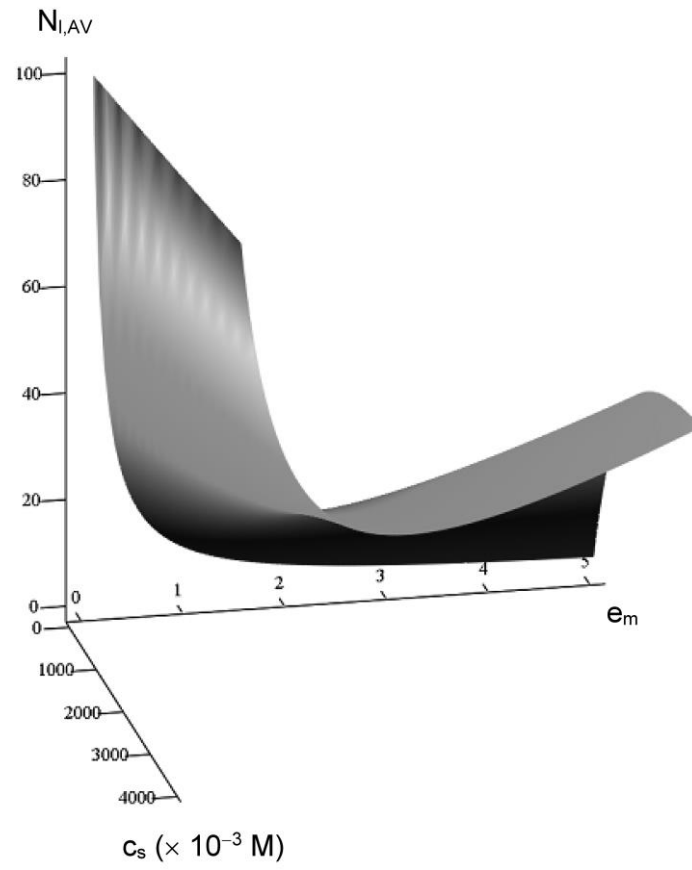


Figure 1. CEC values determined with the ammonium acetate method using different KCl solutions in the final stage of the test and comparison with MB results.

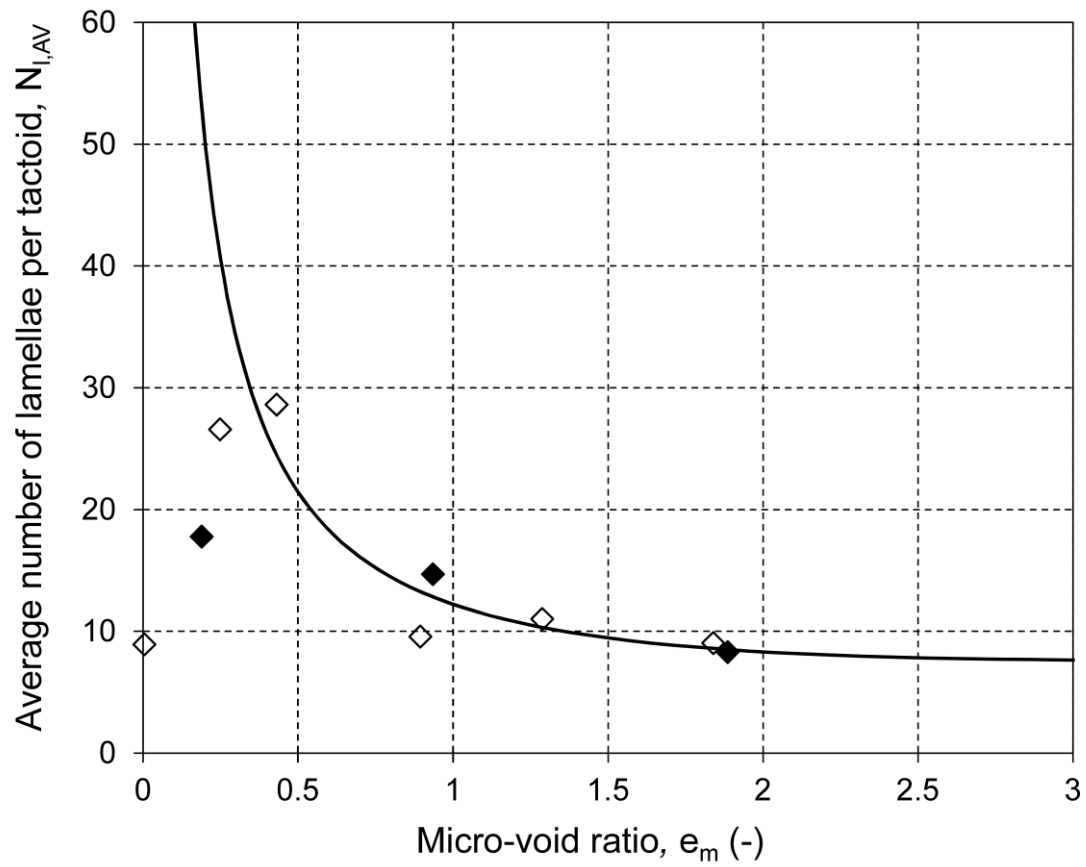


10

11 Figure 2. Plot of the fabric boundary surface (FBS) in the three-dimensional space of the
 12 variables: average number of lamellae per tactoid, $N_{l,AV}$, micro-void ratio, e_m , and salt molar
 13 concentration, c_s .

14

15

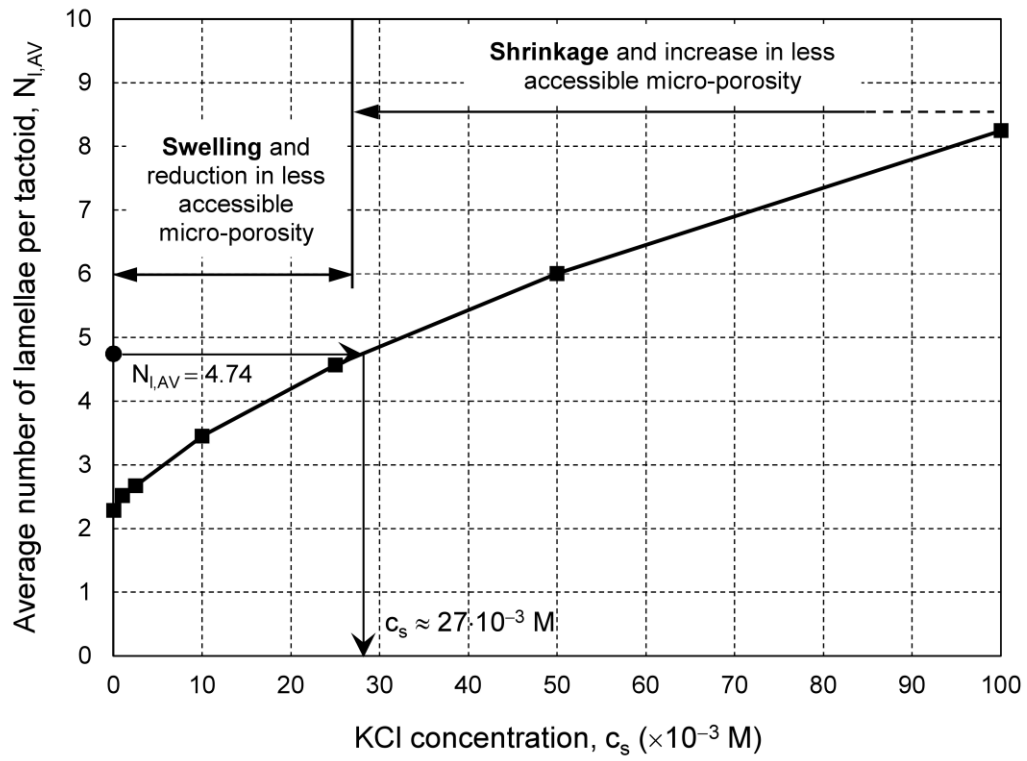


- ◇ $c_s = 0.1$ M - NMR measurements (Data from Muurinen et al., 2013; Ohkubo et al., 2016)
- ◆ $c_s = 0.1$ M - SAXS measurements (Data from Muurinen et al., 2013)

17

18 Figure 3. Comparison between the average number of lamellae per tactoid provided by the
 19 Fabric Boundary Surface (continuous line) and the experimental results taken from the
 20 literature.

21



23

24 Figure 4. Average number of lamellae per tactoid of the bentonite as a function of the
 25 concentration of the extracting KCl solution. The arrows indicate the KCl concentration ($c_s =$
 26 0.027 M) that corresponds to $N_{l,AV} = 4.74$, i.e. the average number of lamellae per tactoid after
 27 the washing phase with isopropanol ($c_s = 0$).
 28

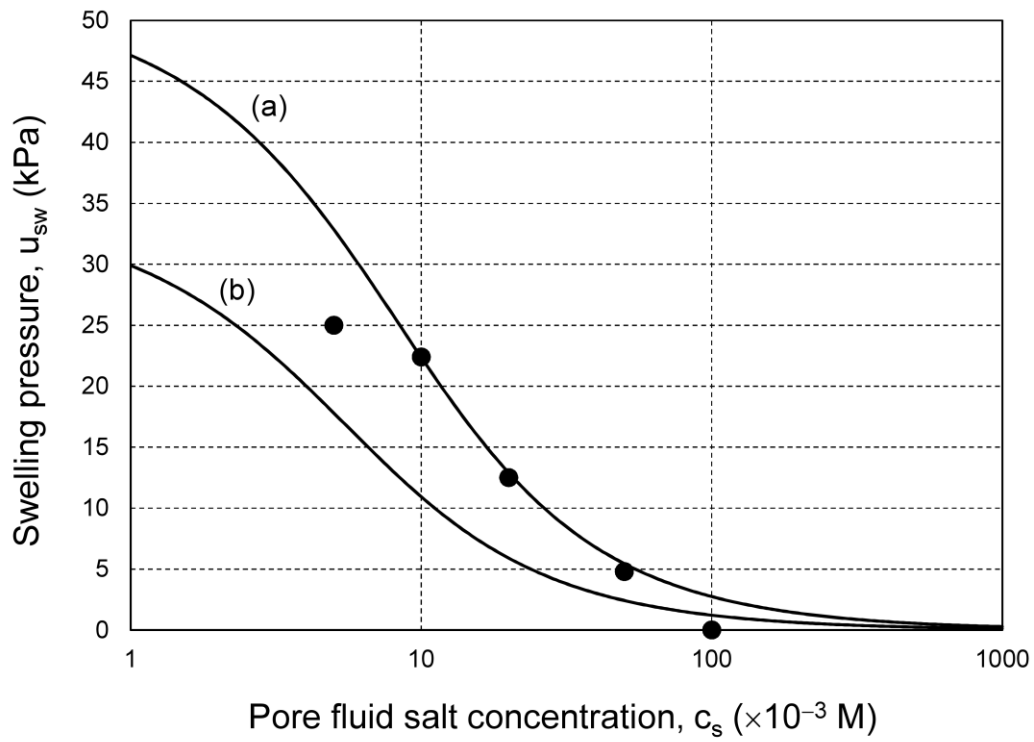


Figure 5. Comparison between the swelling pressure of bentonite, as theoretically predicted on the basis of the average CEC value derived from the methylene blue titration method [curve (a) – CEC = $(97.4 + 104)/2 = 100.7$ meq/100 g] and the standard ammonium displacement method [curve (b) – CEC = $(73.2 + 60.7)/2 = 66.9$ meq/100 g], and the experimental data obtained by Dominijanni et al. (2013) (closed circles).